

Supporting Information

PbSrSiO₄: A New Ultraviolet Nonlinear Optical Material with a Strong Second Harmonic Generation Response and Moderate Birefringence

Shutong Jiang,^a Jinjie Zhou,^a Hongping Wu,^{*a} Hongwei Yu,^{*a} Zhanggui Hu,^a Jiyang Wang^a and
Yicheng Wu^a

^a*Tianjin Key Laboratory of Functional Crystal Materials, Institute of Functional Crystal, Tianjin
University of Technology, Tianjin 300384, China.*

To whom correspondence should be addressed: E-mail: wuhp@ms.xjb.ac.cn

CONTENTS

Experimental	S3
Table S1. Crystal data and structural refinement for PbSrSiO ₄	S5
Table S2. Atoms coordinates, equivalent isotropic displacement parameters.....	S6
Table S3. Selected bond distances (Å) and angles (deg) for PbSrSiO ₄	S7
Table S4. The dipole moments of single PbO ₃ , single SiO ₄ and single SrO ₈	S8
Fig. S1 Experimental and calculated X-ray diffraction patterns of PbSrSiO ₄	S9
Fig. S2 Thermal behaviour of PbSrSiO ₄	S10
Fig. S3 The photograph of the crystal of PbSrSiO ₄	S11
Fig. S4 The IR spectrum of PbSrSiO ₄	S12
Fig. S5 The SHG-weighted electron density maps of the occupied (a) and unoccupied (b) states of PbSrSiO ₄ in the VE process.....	S13
Fig. S6 The photograph of crystal size.....	S14
References	S15

Experimental

Solid-state synthesis

All the reagents including SrCO₃ (Aladdin Reagent Co., Ltd, 98%), PbO (Tianjin Fuchen Chemical Reagent Co., Ltd, 99%) and SiO₂ (Aladdin Reagent Co., Ltd, 99.99%) were used as received. The polycrystalline sample of PbSrSiO₄ was obtained by the high temperature solid state reaction. Stoichiometric reactants of SrCO₃ (1.476 g, 10 mmol), PbO (2.232 g, 10 mmol), SiO₂ (0.601 g, 10 mmol) were ground thoroughly in an agate mortar, and preheated in a ceramic crucible at 500 °C for 10 h. The mixture was cooled to room temperature and ground, then kept at 780 °C for 48 h with several intermediate grindings. By doing these, the pure polycrystalline sample of PbSrSiO₄ was successfully synthesized, and the purity of sample was confirmed by the powder X-ray diffraction (PXRD).

Crystal growth

We used PbO–PbF₂–H₃BO₃ as the flux system to grow single crystals, a mixture of PbO, SrCO₃, SiO₂, H₃BO₃ and PbF₂ at a molar ratio of 1.5:1:1:1:0.5. We thoroughly mixed PbO (3.348 g, 15 mmol), SrCO₃ (1.476 g, 10 mmol), SiO₂ (0.601, 10 mmol), PbF₂ (1.225 g, 5 mmol), H₃BO₃ (0.618 g, 10 mmol) and ground them in an agate mortar. Firstly, the mixture was pressed into a Φ 20 mm × 20 mm platinum crucible in a programmed furnace. To obtain a homogeneous melt, the mixture was heated to 900 °C and held for 15 h. Subsequently, we quickly cooled it to the initial crystallization temperature (852 °C) after a Pt wire placed into the melt, and then the temperature was slowly reduced to 849 °C at a rate of 2 °C per day. By this manner, a few transparent crystals were grown on the Pt wire. And then the crystals were lifted out of the solution and then cooled to 700 °C at a cooling rate of 5 °C h⁻¹, finally, the solution was cooled to the room temperature with the furnace shut down. Some crystals could be artificially picked from the reaction products for the structure determination based on the single-crystal XRD. In addition, a plate-shaped crystal with a size of 2.5 × 2.0 × 0.5 mm³ was used for UV–vis–NIR transmittance spectrum (Fig. 2) measurement.

Powder X-ray diffraction

The PXRD data of PbSrSiO₄ in the angular range of 2θ = 10 °~70 ° were collected on a Bruker D2 PHASER PXRD with Cu-Kα radiation (λ = 1.5418 Å) at room temperature. The scan step width was set as 0.01 ° and a step time was set as 1 s. The experimental data were in excellent agreement with the calculated one (Fig. S1).

Single-crystal X-ray diffraction

The crystal structure of PbSrSiO₄ was determined by single-crystal XRD with Mo Kα radiation (λ = 0.71073 Å) at 293(2) K. A bulk and transparent PbSrSiO₄ crystal was chosen for the crystal data collection. And the data were integrated with a SAINT program.^{S1} The structure was solved and refined by using the SHELXTL system.^{S2} The missing symmetry elements were checked by PLATON.^{S3} Crystal parameters and structure refinements are shown in Table S1. Atomic coordinates, equivalent isotropic displacement parameters are summarized in Table S2. Selected bond distances and angles are listed in Table S3.

IR spectroscopy

IR spectroscopy in the range of 400–4000 cm⁻¹ has been performed on a Nicolet iS50 FT-IR spectrometer. The PbSrSiO₄ sample (~ 9 mg) was measured.

UV Transmittance Spectrum

The Hitachi UV-Vis-NIR spectrophotometer was used to measure the UV-vis-NIR transmittance spectrum (the wavelength range from 240 to 2500 nm) at room temperature.

Birefringence measurement

The birefringence of PbSrSiO₄ was measured through using a cross-polarizing microscope.^{S4} Based on the crystal optics, follow the equation

$$R = \Delta n \times d \quad (1)$$

where R, Δn and d are retardation, birefringence and thickness, respectively.^{S5} Therefore, a triangle PbSrSiO₄ crystal with thickness of 27 μm (Fig. S5) has been used for the birefringence measurement.

Thermal analysis

The thermal behaviors of PbSrSiO₄ were determined using a NETZSCH STA 449C thermal analyzer instrument. About 8.3 mg of PbSrSiO₄ was placed in platinum crucible and heated from room temperature to 1300 °C at a rate of 5 °C min⁻¹ under a constant flow of nitrogen.

Second-harmonic generation measurements

Powder SHG measurements were performed by the Kurtz-Perry method^{S6} with 1064 nm Nd:YAG solid-state laser. Powder samples were ground and sieved into the following particle size ranges: 25–53, 53–75, 75–106, 106–120, 120–150, 150–180 and 180–212 μm, respectively. Microcrystalline KDP with the corresponding size ranges served as the standard.

Theoretical calculations

The electronic structure and optical property of PbSrSiO₄ was calculated by first-principles calculation based on density-functional theory in the CASTEP package.^{S7} During the calculation, the exchange-correlation energy was described by the generalized gradient approximation (GGA)^{S8} with Perdew–Burke–Ernzerhof (PBE)^{S9} functional and Norm-conserving pseudopotential (NCP).^{S10} In PbSrSiO₄, Pb: 5s²5p⁶5d¹⁰6s²6p², Sr: 4s²4p⁶5s², Si: 3s²3p² and O: 2s²2p⁴ were used to valence electrons. The kinetic energy of cutoff was set as 910 eV and 2 × 2 × 1 Monkhorst-Pack^{S11} *K*-point meshes in the Brillouin zones were chosen. The length-gauge formalism derived by Aversa and Sipe^{S12} was used to calculate the SHG coefficients based on the band wave functions at a zero-frequency limit. Lately, Yang, et. al., have developed transform:^{S13}

$$\chi_{\alpha\beta\gamma}^{(2)} = \chi_{\alpha\beta\gamma}^{(2)}(\text{VE}) + \chi_{\alpha\beta\gamma}^{(2)}(\text{VH}) \quad (2),$$

From the above equation, we can see that the total SHG coefficient $\chi^{(2)}$ are divided into two different processes from Virtual-Hole (VH),

Virtual-Electron (VE). The formulas for calculating $\chi_{\alpha\beta\gamma}^{(2)}(\text{VE})$ and $\chi_{\alpha\beta\gamma}^{(2)}(\text{VH})$ are as follows:

$$\chi_{\alpha\beta\gamma}^{(2)}(\text{VE}) = \frac{e^3}{2\hbar^2 m^3} \sum_{vcc'} \int \frac{d^3k}{4\pi^3} P(\alpha\beta\gamma) \text{Im} \left[P_{vc}^\alpha P_{cc'}^\beta P_{c'v}^\gamma \right] \left(\frac{1}{\omega_{cv}^3 \omega_{c'v}^2} + \frac{2}{\omega_{vc}^4 \omega_{c'v}} \right) \quad (3),$$

$$\chi_{\alpha\beta\gamma}^{(2)}(\text{VH}) = \frac{e^3}{2\hbar^2 m^3} \sum_{wvc} \int \frac{d^3k}{4\pi^3} P(\alpha\beta\gamma) \text{Im} \left[P_{vw}^\alpha P_{vc}^\beta P_{cv}^\gamma \right] \left(\frac{1}{\omega_{cv}^3 \omega_{vc}^2} + \frac{2}{\omega_{vc}^4 \omega_{cv}} \right) \quad (4).$$

Here, α, β, γ are Cartesian components, *v* and *v'* denote valence bands, *c* and *c'* refer to conduction bands, and $P(\alpha\beta\gamma)$ denotes full permutation. $\hbar\omega_{ij}$ and P_{ij}^α denote the band energy difference and momentum matrix elements, respectively. In addition, to more clearly and directly display the contribution of electronic orbitals to the SHG effect, the SHG-weighted charge density of the occupied and unoccupied states was determined by a “band-resolved” scheme, and the SHG-weighted density was summed up by the SHG weighted factor and visualized in real space.

Table S1. Crystal data and structure refinement for PbSrSiO₄.

Empirical formula	PbSrSiO ₄
Formula weight	338.90
Temperature	293(2) K
Wavelength	0.71073 Å
Crystal system	orthorhombic
Space group	<i>P</i> 2 ₁ 2 ₁ 2 ₁
Unit cell dimensions	<i>a</i> = 5.7628(7) Å <i>b</i> = 7.2333(7) Å <i>c</i> = 9.7316(11) Å
Volume	405.65(8) Å ³
Z	4
Absorption coefficient (mm ⁻¹)	54.670
F(000)	568
Reflections collected / unique	2211 / 872 [R(int) = 0.0351]
Completeness to theta	100.0 %
Data / restraints / parameters	872 / 0 / 65
Goodness-of-fit on <i>F</i> ²	1.089
Final <i>R</i> indices [<i>F</i> _o ² > 2σ(<i>F</i> _o ²)] ^[a]	<i>R</i> ₁ = 0.0379 <i>wR</i> ₂ = 0.0858
<i>R</i> indices (all data) ^[a]	<i>R</i> ₁ = 0.0402 <i>wR</i> ₂ = 0.0910
Extinction coefficient	0.0021(4)
Absolute structure parameter	0.47(4)
Largest diff. peak and hole	2.298 and -3.098 e·Å ⁻³

^a $R_1 = \frac{\sum ||F_o| - |F_c||}{\sum |F_o|}$ and $wR_2 = \frac{[\sum w(F_o^2 - F_c^2)^2]}{\sum (w(F_o^2)^2)}^{1/2}$ for $F_o^2 > 2\delta(F_c^2)$.

Table S2. Atoms coordinates, equivalent isotropic displacement parameters.

Atoms	x	y	z	U(eq)	BVS
Pb(1)	10497(1)	4385(1)	873(1)	18(1)	1.719
Sr(1)	10183(3)	2510(2)	-2911(1)	4(1)	2.134
Si(1)	9819(8)	4644(5)	4153(5)	6(1)	3.971
O(1)	10320(20)	5561(16)	5665(10)	12(2)	1.920
O(2)	9320(30)	2475(17)	4396(13)	18(3)	2.106
O(3)	7590(20)	5483(19)	3365(14)	15(3)	1.819
O(4)	12160(20)	5000(20)	3228(16)	16(3)	1.976

$U(\text{eq})$ is defined as one third of the trace of the orthogonalized U_{ij} tensor.

Table S3. Selected bond distances (Å) and angles (deg).

Pb(1)-O(2)#1	2.251(13)	O(3)#4-Sr(1)-O(1)#10	75.7(4)
Pb(1)-O(1)#2	2.426(12)	O(4)#2-Sr(1)-O(1)#10	94.8(4)
Pb(1)-O(4)	2.517(15)	O(3)#8-Sr(1)-O(2)#9	112.3(4)
Sr(1)-O(3)#8	2.491(13)	O(4)#6-Sr(1)-O(2)#9	75.3(4)
Sr(1)-O(4)#6	2.534(14)	O(1)#9-Sr(1)-O(2)#9	59.4(4)
Sr(1)-O(1)#9	2.602(11)	O(3)#4-Sr(1)-O(2)#9	85.5(4)
Sr(1)-O(3)#4	2.606(13)	O(4)#2-Sr(1)-O(2)#9	122.2(4)
Sr(1)-O(4)#2	2.610(13)	O(1)#10-Sr(1)-O(2)#9	142.5(4)
Sr(1)-O(1)#10	2.619(11)	O(3)#8-Sr(1)-O(2)#4	143.5(4)
Sr(1)-O(2)#9	2.667(13)	O(4)#6-Sr(1)-O(2)#4	122.0(4)
Sr(1)-O(2)#4	2.786(15)	O(1)#9-Sr(1)-O(2)#4	72.3(4)
Si(1)-O(2)	1.615(13)	O(3)#4-Sr(1)-O(2)#4	57.4(4)
Si(1)-O(3)	1.616(14)	O(4)#2-Sr(1)-O(2)#4	73.4(4)
Si(1)-O(1)	1.637(12)	O(1)#10-Sr(1)-O(2)#4	121.9(4)
Si(1)-O(4)	1.644(14)	O(2)#9-Sr(1)-O(2)#4	69.6(2)
O(2)#1-Pb(1)-O(1)#2	85.7(5)	O(2)-Si(1)-O(3)	106.9(8)
O(2)#1-Pb(1)-O(4)	85.0(5)	O(2)-Si(1)-O(1)	106.8(6)
O(1)#2-Pb(1)-O(4)	72.2(4)	O(3)-Si(1)-O(1)	114.2(7)
O(3)#8-Sr(1)-O(4)#6	92.1(5)	O(2)-Si(1)-O(4)	112.3(8)
O(3)#8-Sr(1)-O(1)#9	78.0(4)	O(3)-Si(1)-O(4)	109.7(7)
O(4)#6-Sr(1)-O(1)#9	124.2(4)	O(1)-Si(1)-O(4)	107.0(7)
O(3)#8-Sr(1)-O(3)#4	155.4(4)	O(1)#9-Sr(1)-O(4)#2	67.9(4)
O(4)#6-Sr(1)-O(3)#4	75.5(4)	O(3)#4-Sr(1)-O(4)#2	109.6(4)
O(1)#9-Sr(1)-O(3)#4	126.6(4)	O(3)#8-Sr(1)-O(1)#10	80.0(4)
O(3)#8-Sr(1)-O(4)#2	76.1(4)	O(4)#6-Sr(1)-O(1)#10	68.8(4)
O(4)#6-Sr(1)-O(4)#2	161.53(10)	O(1)#9-Sr(1)-O(1)#10	154.7(4)

Symmetry transformations used to generate equivalent atoms:

- | | |
|--------------------------|---------------------------|
| #1 $-x+2, y+1/2, -z+1/2$ | #2 $-x+5/2, -y+1, z-1/2$ |
| #3 $-x+5/2, -y+1, z+1/2$ | #4 $x+1/2, -y+1/2, -z$ |
| #5 $-x+2, y+1/2, -z-1/2$ | #6 $x-1/2, -y+1/2, -z$ |
| #7 $-x+3/2, -y+1, z+1/2$ | #8 $-x+3/2, -y+1, z-1/2$ |
| #9 $x, y, z-1$ | #10 $-x+2, y-1/2, -z+1/2$ |
| #11 $x, y, z+1$ | |

Table S4. The dipole moments of single PbO_3 , single SiO_4 and single SrO_8 .

Polyhedron	Dipole moment			Magnitude (Debye)
	x	y	z	
single PbO_3	3.61	5.38	0.79	6.52
single SiO_4	-0.03	-1.52	-0.41	1.57
single SrO_8	-1.64	0.34	3.41	3.80

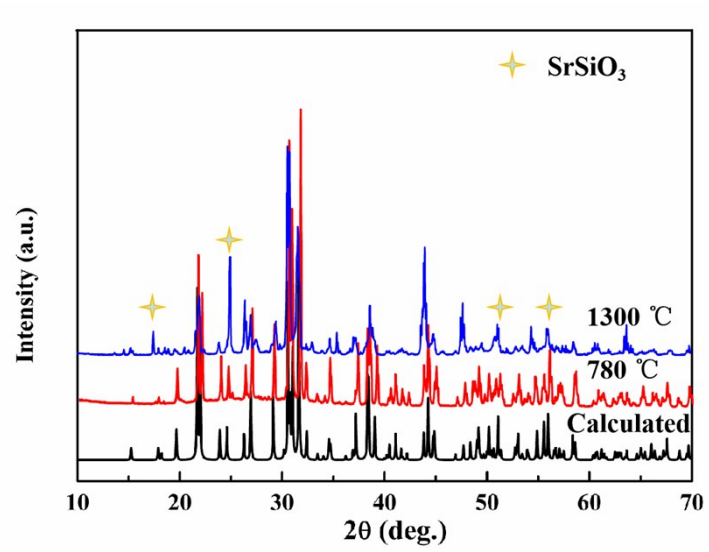


Fig. S1 Experimental and calculated powder X-ray diffraction patterns of PbSrSiO₄.

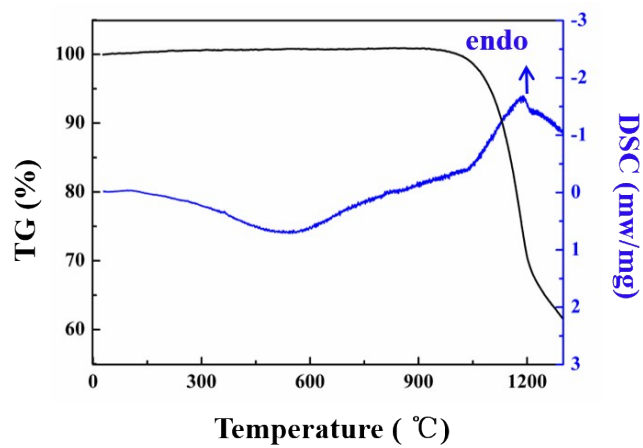


Fig. S2 Thermal behaviour of PbSrSiO_4 .

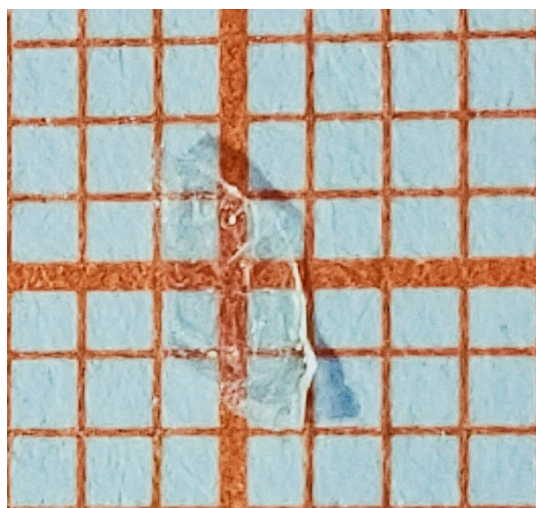


Fig. S3 The photograph of the crystal of PbSrSiO_4 .

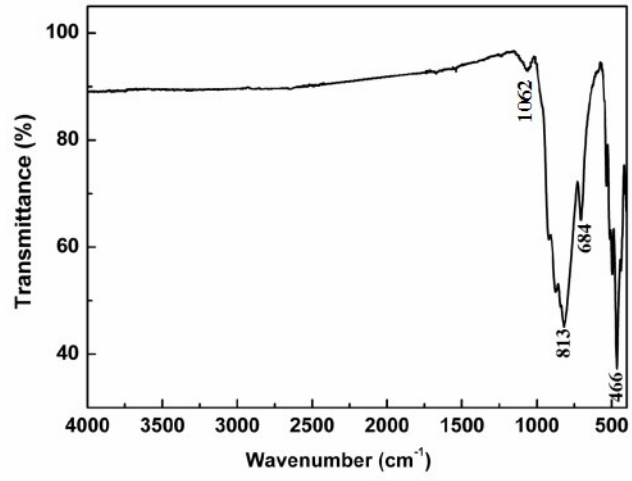


Fig. S4 The IR spectrum of PbSrSiO₄.

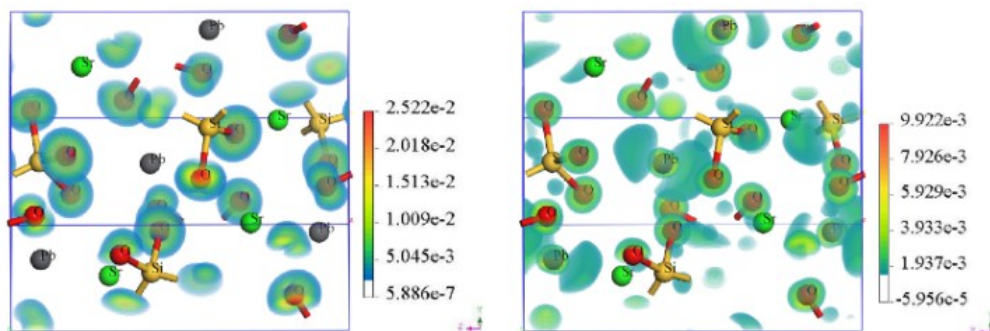


Fig. S5 The SHG-weighted electron density maps of the occupied (a) and unoccupied (b) states of PbSrSiO₄ in the VE process.

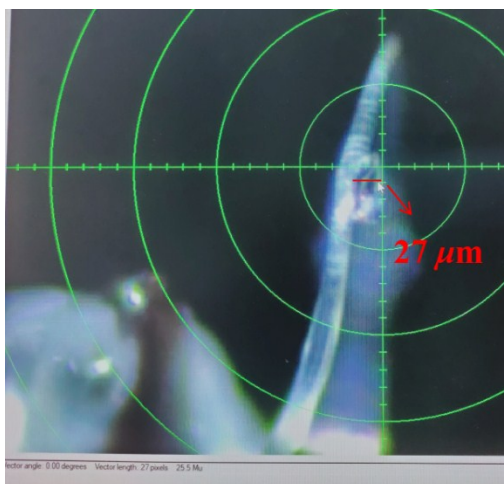


Fig. S6 The photograph of crystal size.

References

- S1. SAINT-Plus, version 6.02A, Bruker Analytical X-ray Instruments, Inc. Madison, WI, 2000.
- S2. G. M. Sheldrick, *Acta Crystallogr. A*, 2008, **64**, 112.
- S3. A. Spek, *J. Appl. Crystallogr.*, 2003, **36**, 7.29
- S4. X. F. Wang, F. F. Zhang, L. Gao, Z. H. Yang and S. L. Pan, *Adv. Sci.*, 2019, 1901679.
- S5. B. E. Sorensen, *Eur. J. Mineral.* 2013, **25**, 5.
- S6. S. K. Kurtz and T. T. Perry, *J. Appl. Phys.*, 1968, **39**, 3798.
- S7. S. J. Clark, M. D. Segall, C. J. Pickard, P. J. Hasnip, M. J. Probert, K. Refson and M. C. Payne, *Z. Kristallogr.*, 2005, **220**, 567.
- S8. J. P. Perdew, J. Chevary and S. Vosko, *Phys. Rev. B*, 1992, **46**, 6671.
- S9. J. P. Perdew, K. Burke and M. Ernzerhof, *Phys. Rev. Lett.*, 1996, **77**, 3865.
- S10. J. P. Perdew, J. Chevary and S. Vosko, *Phys. Rev. B*, 1992, **46**, 6671.
- S11. H. J. Monkhorst and J. D. Pack, *Phys. Rev. B*, 1976, **13**, 5188.
- S12. C. Aversa and J. Sipe, *Phys. Rev. B: Condens. Matter Mater. Phys.*, 1995, **52**, 14636.
- S13. (a) J. Lin, M. H. Lee, Z. P. Liu, C. T. Chen and C. J. Pickard, *Phys. Rev. B: Condens. Matter. Phys.*, 1999, **60**, 13380; (b) B. B. Zhang, M. H. Lee, Z. H. Yang, Q. Jing, S. L. Pan, M. Zhang, H. P. Wu, X. Su and C. S. Li, *Appl. Phys. Lett.*, 2015, **106**, 031906.